Journal of Glaciology, Vol. 43, No. 145, 1997

Distribution and fall-out of ^{137}Cs and other radionuclides over Antarctica

M. Pourchet,[1] S. K. Bartarya,[2] M. Maignan,[3] J. Jouzel,[4] J. F. Pinglot,[1] A. J. Aristarain,[5] G. Furdada,[6] V. M. Kotlyakov,[7] E. Mosley-Thompson,[8] N. Preiss,[1] N.W. Young[9]

[1]*CNRS, Laboratoire de Glaciologie et Géophysique de l'Environnement, 38402 Saint-Martin-d'Hères Cedex, France*

[2]*Wadia Institute of Himalayan Geology, Dehra Dun 248001 (U.P.), India*

[3]*Universite de Lausanne, Instituts de Minéralogie et de Mathématiques, CH-1015 Lausanne, Switzerland*

[4]*Laboratoire de Modélisation du Climat et de l'Environnement, CEA/DSM CE Saclay, 91191 Gif-sur-Yvette, France*

[5]*CRICYT, Instituto Antártico Argentino, 5500 Mendosa, Argentina*

[6]*Departamento Geologia Dinàmica, Geofisica i Paleontologia, Universitat de Barcelona, Zona Universitària Pedralbes, 08028 Barcelona, Spain*

[7]*Academy of Sciences, Institute of Geography, Moscow 109017, Russia*

[8]*Byrd Polar Research Center, The Ohio State University, Columbus, Ohio 43210, U.S.A.*

[9]*Antarctic CRC, University of Tasmania, Hobart, Tasmania 7001, Australia*

ABSTRACT. This article aims to give a comprehensive view of the distribution patterns for natural and artifical radionuclides over Antarctica. We focus this study on ^{137}Cs, ^{210}Pb and tritium. Applying various statistical methods, we show that the deposition of radionuclides reveals a structured distribution, although local drift redistribution and the snow-surface roughness disturb the representativeness of samples and produce a "noise" effect. The deposition of ^{137}Cs over Antarctica (885 TBq) represents 0.09% of the total deposition of this radionuclide in the world and the correlation between ^{137}Cs fluxes and accumulation shows two sub-populations. For the stations with a mean annual temperature above −21 °C, a strong correlation is found, whereas the correlation is lower for locations with temperatures below −21 °C. The flux of ^{210}Pb varies from 0.9 to 8.2 Bq $m^{-1}a^{-1}$ with values strongly correlated with the accumulation and a well-defined spatial structure. The same mechanism governs the deposition of artificial and natural tritium but it clearly differs from that of other radionuclides associated with particulate material. The "dry fall-out" accounts for between 60 and 80% of the total fall-out for the artificial radionuclides and around 40% for ^{210}Pb. This difference is likely related to a tropospheric fraction for ^{210}Pb. Despite its isolated location, the radioactive fall-out of artificial long-lived radionuclides over Antarctica has been ten times greater than for natural radionuclides.

1. INTRODUCTION

A series of atmospheric thermonuclear tests during the period 1953–80, mostly in the Northern Hemisphere, has injected large quantities of artificial radionuclides into the upper atmosphere and stratosphere. These radionuclides have been transported from their sources over Antarctica. During their transport, they are subject to usual removal processes. Because of the well-known arrival dates, they serve as characteristic reference levels in snow and are currently used in glaciological studies to determine the average rate of snow accumulation over the last 40 years. The artificial and natural radionuclides present in the ice sheets of the polar regions have also been widely used as atmospheric tracers to understand the transport and circulation of continental, tropospheric and stratospheric air masses (Wilgain and others, 1965; Feely and others, 1966).

The behavior of fission products depends upon the latitude, the altitude and the season when they were released. Fission products introduced into the equatorial stratosphere spread rapidly in their latitudinal band of injection but migrate slowly towards the pole (Picciotto and Wilgain, 1963). The concentration of these artificially produced radionuclides in Antarctic and sub-Antarctic areas is controlled by their long-range transport from mid-latitudes. For tropospheric transport, a 30 day transit time of the air masses from distant continental regions to the South Pole has been suggested by Maenhaut and others (1979).

Thus, the use of airborne radionuclides as atmospheric tracers had been demonstrated (Junge, 1963; Rama, 1963; Lambert and others, 1966, 1983; Kolb, 1970; Luyanas and others, 1970; Poet and others, 1972; Telegadas, 1972; Moore and others, 1973; Reiter, 1978; Maenhaut and others, 1979). However, after reaching Antarctica, the process of deposition or fall-out of these radionuclides is not uniform and the factors controlling their deposition or spatial distribution and the roles of accumulation, wind and local topographic conditions are not completely understood.

In recent years, studies have been made to elucidate the spatial and temporal variation of snow accumulation and their dependence on temperature, altitude, distance to the coast (Young and others, 1982; Pettre and others, 1986; Giovinetto and others, 1990; Goodwin, 1991) as well as the effect of katabatic wind and cyclonic activity on snow accu-

https://doi.org/10.3189/S0022143000035024 Published online by Cambridge University Press

mulation (Goodwin, 1990; Morgan and others, 1991). The sparse data for specific radionuclides have restricted studies to determine their detailed spatial variations and to examine factors responsible for these variations such as processes of deposition (dry or wet). Existing mapping of radionuclide fall-out over Antarctica and studies related to spatial correlations can still be considered as preliminary. The present paper aims to give a comprehensive view of the distribution pattern for natural and artificial radionuclides over Antarctica. An attempt has also been made to compute the total budget of ^{137}Cs fall-out, from 1955 to 1980.

2. MATERIAL AND METHODS

After melting and filtration (Delmas and Pourchet, 1977), snow samples obtained from different stations in Antarctica (Fig. 1) have been analysed for total beta activity over several years using low-level counting equipment (Pinglot and Pourchet, 1979). The filters were later combined together for each station. They were then analysed by gamma spectrometry using a specially designed low-background scintillation detector (Pinglot and Pourchet, 1994) in order to identify, for each site, the total content of caesium and other radio-isotopes from the nuclear bomb tests, together with the natural radioactivity. The available data of total fall-out of ^{137}Cs, ^{90}Sr, ^{3}H and other radionuclides and fluxes of ^{210}Pb, which have been compiled (from Lambert and others, 1983; Sanak, 1983; Bendezu, 1978; Jouzel and others, 1979; Koide and others, 1979, 1981; Raisbeck and others, 1981, 1987, 1990, and various other sources) or generated by us, are given (Table 1a and b). The specific activities have been corrected for decay to the deposition time. The precision of our measurement is about 20% for ^{137}Cs, ^{210}Pb and about 100% for ^{41}Am, ^{226}Ra and ^{234}Th.

In Antarctica, the physical variables, accumulation, temperature, altitude and distance to the coast are strongly linked (Young and others, 1982; Pettre and others, 1986). We have first correlated the radionuclides distribution with the accumulation, because it was anticipated that the wet deposition, directly related to the accumulation, has a strong influence on the radioactive fall-out. To complement this approach, spatial geostatistical investigations have been performed on the set of radionuclides data applying different methods used for measuring the spatial correlation. Mainly variograms, which represent the half mean-square differences of grades (Equation (1) in which x is the spatial coordinate) and correlograms, i.e. the correlation coefficient between measurements for each lag h (Equation (2)), were for a variable T, established:

$$\text{Gamma}\,(h) = \frac{1}{2}(T(x+h) - T(x))^2 \quad (1)$$

$$\text{Cor}\,(h) = \text{Cov}\,T(x+h)T(x)/(T(x+h)).(T(x)). \quad (2)$$

As a verification process, we note that the variographic analysis of altitudes, in using the same location as the stations with radionuclide measurements, shows no nugget effect (this means exact measurements without variability at very small distances), and that it is easy to fit experimental variograms. The adjustments to Gaussian models show the long-distance drift in directions 45°, 75° and allow adjustments in directions 45° and 135° for distances, respectively, up to 1600 and 970 km. This is, of course, related to the altitudes as indicated only for the 78 samples and cannot be generalized for the whole elevation map. Since the mountain ranges are structures which extend over large distances and almost always show spatial correlations (clustering of high peaks, no systematic alternation of one high summit and one low summit), the well-shaped variograms for the elevation gives confidence to the quality of the measurements. Moreover, the presence of a nugget effect (non-zero variance for very small distances) would have revealed possible errors of measurements; this is not the case.

The variographic analysis of temperatures shows the same anisotropy as for altitudes. All variograms show no nugget effect, which indicates a high degree of accuracy of the measurements and no variation at small distances.

The spatial correlation of accumulation shows an important anisotropy in the direction NNE75 and SSW165, which can be interpreted as directly related to the elevation edge with the same orientation. To underline that the mountain range brings a rather sudden increase of elevation, we here extend the term of "scarp edge" to "elevation edge" in order to characterize the influence of the accumulation (i.e. long-range correlation along the mountain range and short-range correlation across the mountain range). This physical variable shows some nugget effect in some directions like direction 075°, thus indicating a residual variability at a small scale but not in the direction 165°.

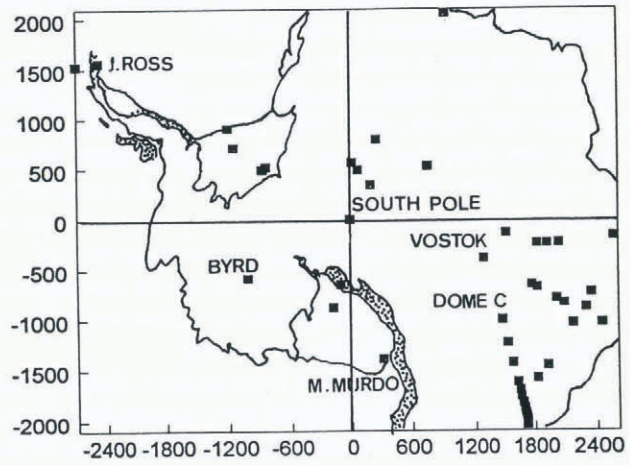

Fig. 1. Map of Antarctica showing locations of ice-coring stations.

3. RESULTS

The fluxes of radionuclides, at a given location in Antarctica, depend on the concentration in the atmosphere, the source region, stratosphere–troposphere exchanges, transport and deposition processes (i.e. either wet or dry deposition) and post-depositional changes. Recent snow cover (less than 50 years) is currently dated by the total beta radioactivity. The first significant increase of radionuclide content was observed in January 1955 (Picciotto and Wilgain, 1963) and corresponds to the arrival of the Yvy and Castle series tests conducted in 1953. This increase in total beta activity due to artificial radionuclides, mainly ^{137}Cs and ^{90}Sr, is about 20 times higher than the natural activity level, mainly due to ^{210}Pb. The highest recorded activity was in 1965 and must have resulted from the stratospheric transfer of debris from the Dominic and U.S.S.R. test series. The short-term temporal variations in fall-out of radionuclides have been discussed by many workers (Wilgain and others, 1965; Lambert and others, 1977, 1990; Merlivat and others,

https://doi.org/10.3189/S0022143000035024 Published online by Cambridge University Press

Table Ia. Major radionuclide fall-out or flux, geographical and meteorological parameters for coring stations

Station	Lat. S	Long. E	Alt.	Temp.	Accum.	^{137}Cs	^{90}Sr	^{210}Pb	T	No.
	0°	0°	m	°C	kg m^{-2} year^{-1}	Bq m^{-2}	Bq m^{-2}	Bq m^{-2} year^{-1}	T U M W	
M.M	77.83	167	20		160			6.9[4]		30
J9	82.37	191.33	50	−29.4	90	89	96[1]	1.9[1]	211[1]	31
F9	84.4	189	50	−30.4	84	17				32
K105	67.58	93.70	1351		313	132				33
VK 631	72.22	96.62	3421		68	52				34
Komso	74.10	97.50	3498	−53.9	64	52		1.16[5]		35
vk747	73.25	97.07	3270		84	40				36
VK 17	78.45	106.84	3470	−55.4	19	35				37
DB	76.92	95.17	3400		32	174				38
Vostok	78.45	106.84	3471	−55.4	23	58				39
BHD	66.73	112.83	1315		631	59				40
BHDB	66.73	112.83	1315		631	81				41
GC 38	70.44	11.74	2524	−38.9	121	50				42
GC 40	71.17	111.36	2695	−43.6	126	55				43
GC 47	73.70	110.20	3046	−52.1	45	36				44
GD 03	69.00	115.48	1832	−29.4	476	78				45
GD 12	68.98	126.93	2170	−32.6	350	95				46
GD 15	69.00	130.81	2150	−33.3	356	100				47
GF 01	68.50	110.85	1800	−28.7	367	63				48
GF 04	68.53	107.24	2120	−32.7	293	46				49
GM 13	73.17	110.45	2960	−52.9	65	59				50
JRF	64.25	302.25	1690	−13.4	163	32				51
JRG	64.25	302.25	1350	−11.3	236	40				52
PS 9	90.00	90.00	2800	−50.7	80	52				53
PS 10					80	46				54
PS 15					79	40		1.64		55
PS 16					86	45				56
PS 18					80	74				57
PS 19					73	67				58
PS 20					81	97				59
PS 21					79	28				60
PS 22					79	36				61
PS 74					84	41				62
PS 77					80	59				63
PS 78					79	51				64
PS					80		144[3]	1.89[4]	720[2]	65
New Byrd	80.0	240.0	1500		180			5.5[4]		66
R. Boudouin	70.43	24.32	20		400			8.2[4]		67
2-11-279	82.9	18.2	2610	−49.2	36			1.1[4]		68
1-15-415	85.2	1.6	2630	−48.6	61			1.9[4]		69
1-13-370	85.8	8.7	2690	−50.0	42			1.2[4]		70
1-10.275	86.6	30.6	2860	−47.9	55			1.4[4]		71
2-0-0	82.1	55.1	3720		31			0.9[4]		72
Livingston Is.	62.67	299.62	265	−4	681			6.7		74
D 136	77.16	307.1	50	−23.8	189				586[12]	75
BAS 5	81.47	299.40	125	−28.6	89				600[12]	76
BAS 6	81.60	301.83	130	−28.7	92				495[12]	77
D 336	78.75	302.1	70	−26.1	156				452[12]	78
DDu	66.7	139.8	43	−10.7	140			3.8[4]		73
A 3	66.69	139.82	190	−14.3	220			4.77[5]		1
D 9	66.70	139.82	223	−15	250			5.0[5]		2
D 12	66.70	139.78	246	−15.3	350	63				3
D 23	66.73	139.62	556	−17.5	440	88				4
D 26	66.77	139.55	589	−17.9	275	44				5
D 33	66.80	139.43	690	−18.3	139	26				6
D 41	66.90	139.21	924	−19.8	600				840[2]	7
D 42	66.99	139.11	1028	−22	320	65				8
D 43	67.06	139.01	1143	−22.6	240	52				9
D 45	67.22	138.83	1353	−24	420		227[3]	6.63[3]		10
D 47	67.39	138.64	1524	−25.8	260	78				11
D 50	67.62	138.33	1709	−27.6	240		102[3]	2.69[3]	430[2]	12
D 53	67.86	137.99	1898	−29.8	360	125				13
D 55	68.03	137.78	1995	−31.1	70	20				14
D 59	68.34	137.31	2228	−34.3	320		198[3]	4.76[3]	720[2]	15
D 60	68.45	137.20	2291	−36.3	260	56				16
D 66	68.94	136.49	2357	−38.8	200		181[6]			17
D 72	69.44	135.76	2412	−41.2	230		107[3]	2.49[3]		18
D 80	70.02	134.82	2487	−41.4	240	92	194[3]	5.23[3]	620[2]	19
D 100	71.56	131.97	3100	−46.3	130		145[6]	2.17[5]	500[2]	20
D 120	73.06	128.74	3280	−52.3	80			1.33[5]	250[2]	21
DC a	74.64	124.17	3240	−53.5	32				470[2]	22
DC b					35	36		1.07		23
DC 5					34	29				24
DC 15					32	61				25
DC 16					37	56				26
DC 18					36	54				27
DC 80					32	44				28

https://doi.org/10.3189/S0022143000035024 Published online by Cambridge University Press

Table 1b. Minor radionuclide fall-out or flux. Source of data: present study for data without brackets, otherwise [1]Koide and others, 1979; [2]Jouzel and others, 1979a; [3]Lambert and others, 1983; [4]Crozaz, 1967, 1969; [5]Sanak, 1983; [6]Bendezu, 1978; [7]Raisbeck and others, 1987; [8]Raisbeck and others, 1981; [9]Raisbeck and others, 1990; [10]Koide and others, 1981; [11]Cutter and others, 1979; [12]Graf and others, 1994

Station	Accum.	^{238}Pu	$^{239+240}Pu$	^{241}Pu	^{241}Am	^{10}Be	^{226}Ra	^{234}Th	No.
	kg m^{-2} year^{-1}	Bq m^{-2}	Bq m^{-2}	Bq m^{-2}	Bq m^{-2}	× 10^{9}At m^{-2} year^{-1}	Bq m^{-2} year^{-1}	Bq m^{-2} year^{-1}	
DC	32	0.24[11]	1.0[10]	15.1[10]		1.57[7]			22
DC	35				0.42		0.082	0.012	23
DC	32		1.51[11]						29
J9	90	0.52[1]	1.5[1]	16.3[1]					31
Vostok	23					2.0[8]			39
PS15	79				0.96				55
PS	80					2.7[9]			65

1977; Jouzel and others, 1979b; Koide and others, 1979; Maenhaut and others, 1979). Here, we will therefore discuss spatial distributions of total fall-out of artificial radionuclides covering the total duration of atmospheric nuclear tests and fluxes of natural radionuclides.

Table 1 shows significant variation in the rate of accumulation, temperature, altitude and fall-out of radionuclides. For example, while the rate of accumulation varies by a factor of 30, the fall-out of ^{137}Cs (between 1955 and 1980) varies by a factor of no more than 17, and the ^{210}Pb fluxes by a factor of six which suggests a significant influence of depositional processes on radionuclide fluxes.

The characteristics of radioactive fall-outs are not examined for the various radionuclides.

a. ^{137}Cs

Over all of Antarctica the total fall-out of ^{137}Cs for the whole deposition time (1955–80) varies from 17 Bq m^{-2} (Ross Ice Shelf, station F9) to 174 Bq m^{-2} (DB). It follows a log-normal distribution, with a tail for high values above 120 Bq m^{-2}. The median of 54 Bq m^{-2} lies 10% below the mean value of 60.2 Bq m^{-2} revealing an asymmetry in the distribution. The three highest values, largely above the other samples, are located at D53, K105 and DB and appear as outliers. The data fit well on a half-normal probability plot. Mean values obtained from diverse geographical areas are not significantly different:

Location	Mean value	Standard deviation	No. of samples
	Bq m^{-2}		
Dumont d'Urville–Dome C axis	63	29	17
Casey–Vostok axis	66	20	12
Mirny–Vostok axis	78	53	7
South Pole Station	53	19	13
Dome C station	47	12	6

Along the Dumont d'Urville–Dome C (DDu–DC) axis, which possesses the highest number of values, the total fall-out is linked with the accumulation by relation (3), which is significant at the 99% confidence level ($\rho = 0.65$):

$$Y\ (\text{caesium}) = 0.12X\ (\text{accum}) + 35.5\,. \qquad (3)$$

The extrapolation for null accumulation gives an estimate of ^{137}Cs "dry deposition" of 35.5 Bq m^{-2}. In this region, the dry deposition would thus represent 56% of the total deposition of ^{137}Cs. The linear regression of ^{137}Cs vs accumulation for all samples yields a constant value (interpreted as dry deposition) of 49 Bq m^{-2} and a regression coefficient of 0.0649 ^{137}Cs per unit of accumulation ($\rho = 0.34$). The mean value of dry deposition represents for all samples 82% of the total deposition. The relatively low correlation may be due to:

(i) The dispersion of the data values. The dispersion of these values is caused by the fact that the meteorological regimes differ from place-to-place.

(ii) The accuracy of accumulation and deposition measurements. The uncertainty in the accumulation measurement can be generally neglected compared to the uncertainly of ^{137}Cs measurements.

(iii) The sampling representation, because the sampling corresponds, both for ice cores and pits, to a small section and the representation strongly depends upon the local relief (sastrugi, dunes) and the drift redistribution. At two stations, South Pole (SP) and Dome C (DC), the magnitude of effects (ii) and (iii) has been estimated. For these two stations with 13 and six sampling sites, respectively, the standard deviation is around 30% (34% and 23%, respectively).

Using different complementary methods, we now examine the statistical properties of the ^{137}Cs distribution.

No global correlation appears on the scatter plot of ^{137}Cs vs temperature, with the exception that two sets are totally separated: temperatures less than −50°C and temperatures over −35°C with seven samples between these two sets. These two sets, and the intermediate group of seven samples appear also separated on the scatter plot of ^{137}Cs vs accumulation with a global linear correlation of 0.34.

The scatter plots of ^{137}Cs vs accumulation, conditioned by temperature, reveal the correlation coefficients and the regressions for the different sub-populations. The conditioning yields increasing correlation coefficients for ^{137}Cs vs accumulation with a three-fold filtering of temperature (Fig. 2): 0.48 for temperatures below −38.3°C, 0.58 for temperatures between −38.3° and −26°C and 0.86 for temperatures above −21°C. This is confirmed by another filtering accord-

https://doi.org/10.3189/S0022143000035024 Published online by Cambridge University Press

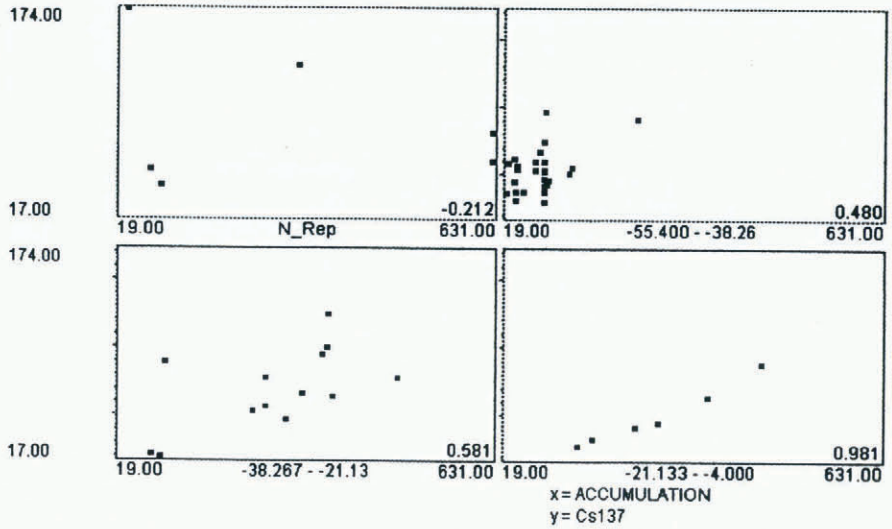

Fig. 2. Bivariate graphs of ^{137}Cs vs accumulation, conditioned (filtered) by temperature. The first scatter plot is Nrep (i.e. not-represented) for observations where no temperature data are available. The other graphs show the behaviour of ^{137}Cs (vertical) vs accumulation (horizontal). The correlation coefficient is indicated in the bottom-right corner. These graphs were obtained for iso-amplitude and for iso-frequency conditioning.

ing to five values of temperatures with tentatively equal frequencies:

Temperatures °C	*Coefficients of correlation*
−55.4 to −52.1	0.27
−52.1 to −50.0	−0.14
−50.0 to −32.7	0.54
−32.7 to −23.8	0.60
−23.8 to −4	0.97

Two strictly different populations appear when conditioning the relationship of ^{137}Cs and accumulation by temperature. For temperatures below −50.7°C, no significant correlation can be obtained, whereas for temperatures above −50.7°C linear behaviours are obvious. Thus, the regression coefficients diminish when temperature increases.

The statistics of ^{137}Cs vs classes of accumulation show an increase of grade without the assumption of linearity expressed by correlation:

Accumulation kg m^{-2} year^{-1}	*^{137}Cs mean value* Bq m^{-2}	*^{137}Cs standard deviation* Bq m^{-2}
19–45	58.30	40.02
45–80	47.73	15.36
80–163	50.25	22.42
163–313	60.16	29.61
313–631	81.70	19.83

A trivariate graphical representation of ^{137}Cs vs temperature and accumulation shows, in three dimensions, the piecewise linear behaviour found in the categorized analysis (Fig. 3).

A principal-component analysis performed considering the temperature, accumulation and ^{137}Cs (Fig. 4) extracts 66% of the total variance on the first inertia axis and 95% on the plane 1–2. The observations are clearly split in a compact group, with low temperature and low accumulation, and a scattered group correlated positively with the temperature and the accumulation (with the exception of samples D55, F9, GC38, GC6 and PS20). These groups are not separated when projected on to the ^{137}Cs vector. The principal-component analysis repeated with the addition of variable altitude confirms the same splitting into two groups.

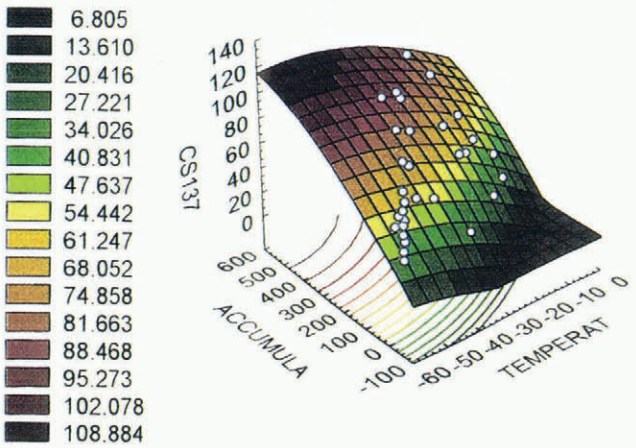

Fig. 3. Quadratic surface for temperature vs accumulation and ^{137}Cs.

The hierarchical ascending classification (Fig. 5) clarifies the split obtained by the factorial analyses. Two groups, A and B, are obtained which are specifically related to the localization and the snow accumulation. A first group shows the sampling points in the vicinity of Dumont d'Urville and from there on a line parallel to the eastern coast. The second group includes the sampling sites on the polar plateau.

^{137}Cs	*Group A: coastal*	*Group B: plateau*
Mean value	60.0 Bq m^{-2}	51.9 Bq m^{-2}
Standard error	5.3 Bq m^{-2}	4.1 Bq m^{-2}

https://doi.org/10.3189/S0022143000035024 Published online by Cambridge University Press

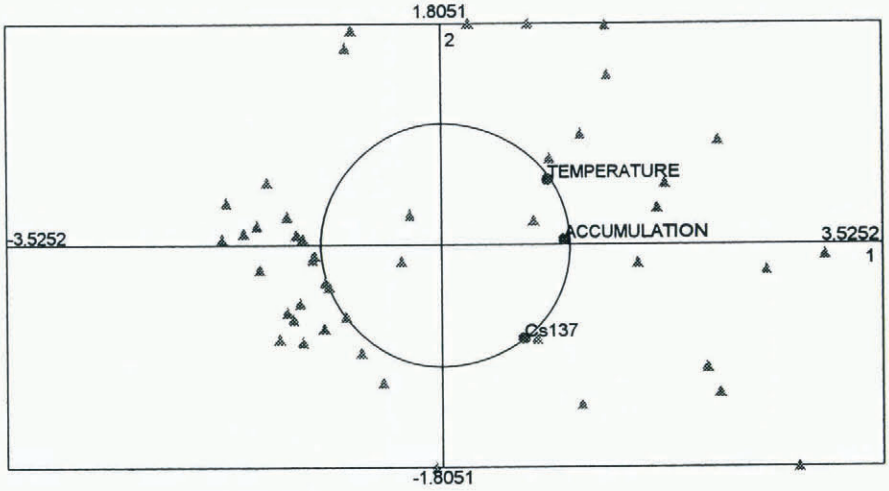

Fig. 4. Principal component analysis (PCA) on the variables of temperature, accumulation and ^{137}Cs.

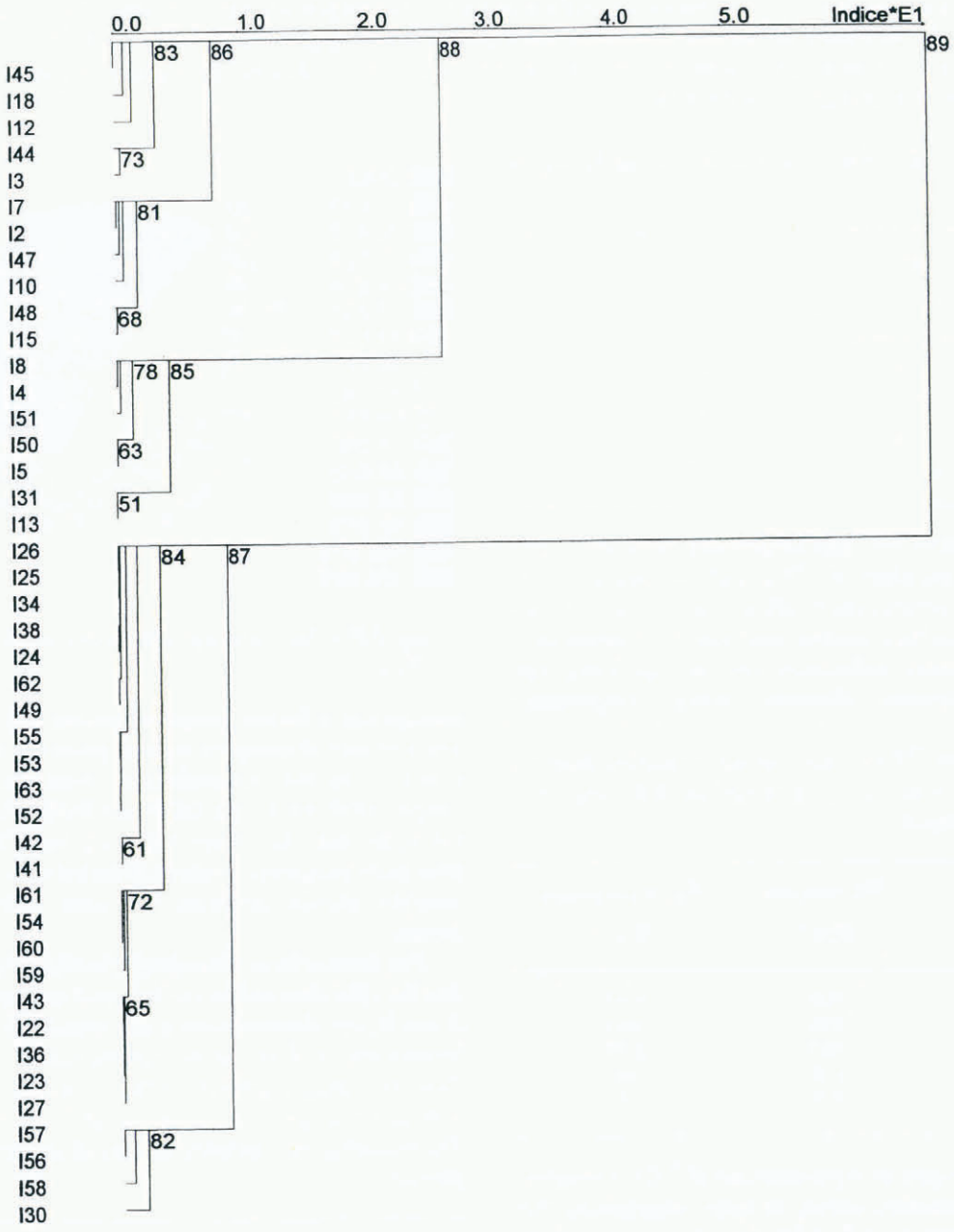

Fig. 5. Hierarchical ascending classifications on three variables: accumulation, temperature and ^{137}Cs. The classification of observations and their relevant clustering is shown in sub-groups. The height of the dendogram is the measure of the "classification distance" among the elements. IXX designates I for individual, with XX being the row numbers, as shown in Table 1 with the raw data.

https://doi.org/10.3189/S0022143000035024 Published online by Cambridge University Press

The correlation matrices show inversion of correlation coefficients for ^{137}Cs for these two groups:

Group A: coastal				*Group B: plateau*			
Alt.	*Temp.*	*Accum.*	^{137}Cs	*Alt.*	*Temp.*	*Accum.*	^{137}Cs
1	−0.64	0.11	0.35	1	−0.91	−0.53	−0.47
	1	0	−0.31		1	0.66	0.41
		1	0.74			1	0.25
			1				1

The relationship of ^{137}Cs vs altitude and temperature inverts between the two groups and the correlation vs accumulation drops drastically from the coast to the plateau locations. The regression lines are different from group A (coastal, Equation (4)) and B (plateau, Equation (5)):

$$Y\,(\text{caesium}) = 0.193 \times (\text{accum.}) + 7.12 \qquad \rho = 0.74 \quad (4)$$

$$Y\,(\text{caesium}) = 0.145 \times (\text{accum.}) + 42.35 \qquad \rho = 0.25\,. \quad (5)$$

Within group B, the average ^{137}Cs is 45.4 Bq m^{-2} for accumulation below 50 kg m^{-2} a^{-1} which is consistent with the previous estimation of "dry deposition".

The omnidirectional variogram (Fig. 6a) is consistent with a spherical model with a 450 km range. In directions NW150 and NE45, directional variograms can be fitted with exponential models with ranges of 850 and 575 km.

The isoline maps of radionuclides show large-scale structures which must not be interpreted as smooth as it may appear as this is due to the limited number of samples available. The ^{137}Cs map, established on the basis of square blocks 250 km × 250 km (Fig. 7), shows a significant increase on the eastern border, reaching 100 Bq m^{-2}, and a peak for DC. In this quadrant, the ^{137}Cs map is somewhat similar to a rough map of the elevation gradient. The ^{137}Cs fall-out is above 90 Bq m^{-2} for 14 squares, or 875 000 km^2. Fourteen squares on the plateau (875 000 km^2) have a value lower than 50 Bq km^{-2}; 44 blocks, i.e. 2 750 000 km^2, have estimated values of ^{137}Cs between 60 and 80 Bq m^{-2}.

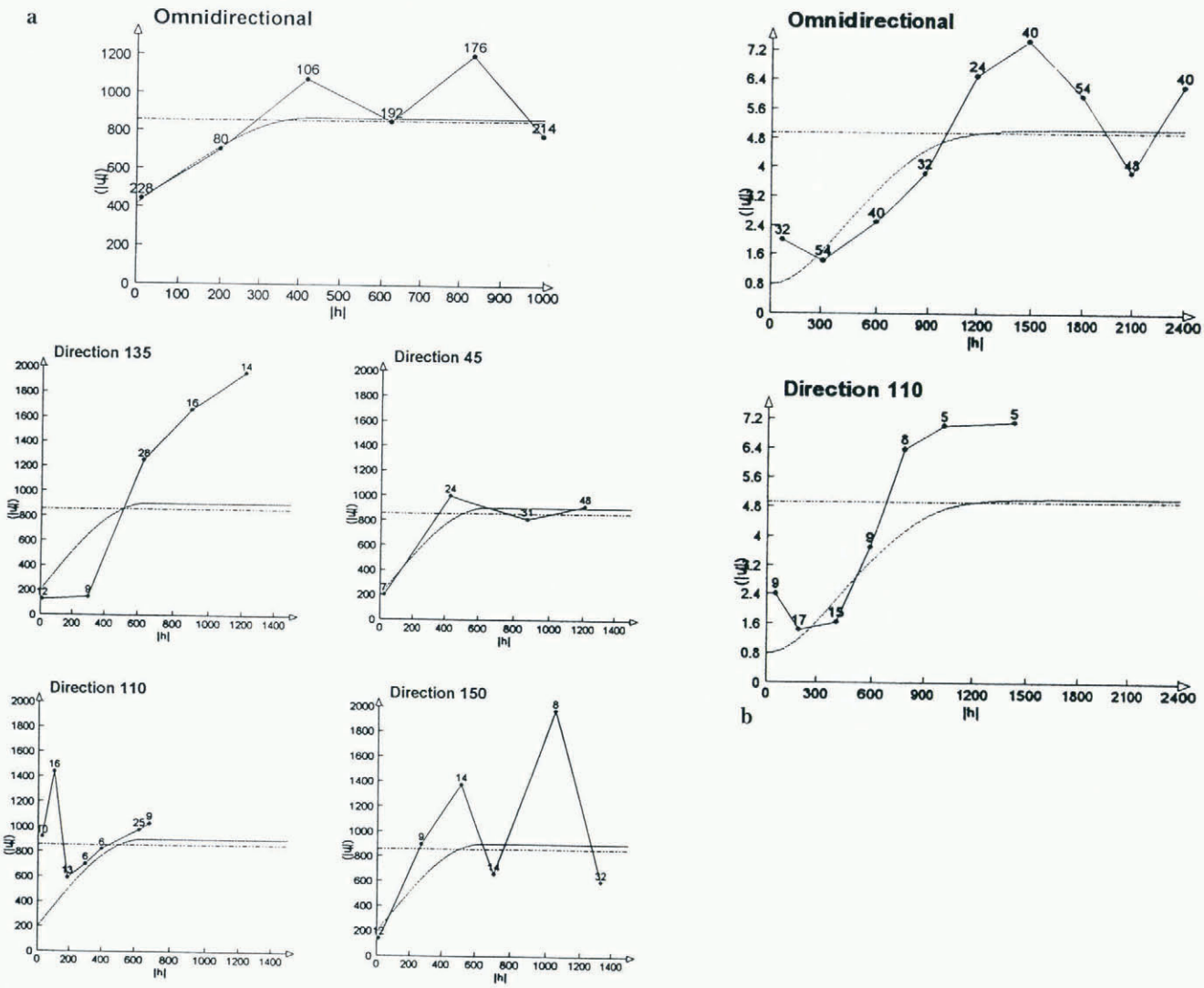

Fig. 6. Omnidirectional variograms for ^{137}Cs (a) and ^{210}Pb (b). The variogram depicts the correlation as a function of distance. On a variogram, one can read the global fit of a model (curve) to the experimental values for given distances (the straight lines). The horizontal line is the statistical variance, i.e. the variance without spatial correlation. It is reached for a distance called the "range", which is a measure of the zone of influence. Beyond this range, data measurements are spatially independent. The intersection of the model curve with the vertical axis represents the residual variance between measurements for a very small distance. It is called the "nugget effect" and represents the residual variability of the data which cannot be removed even with sampling on a very dense grid.

https://doi.org/10.3189/S0022143000035024 Published online by Cambridge University Press

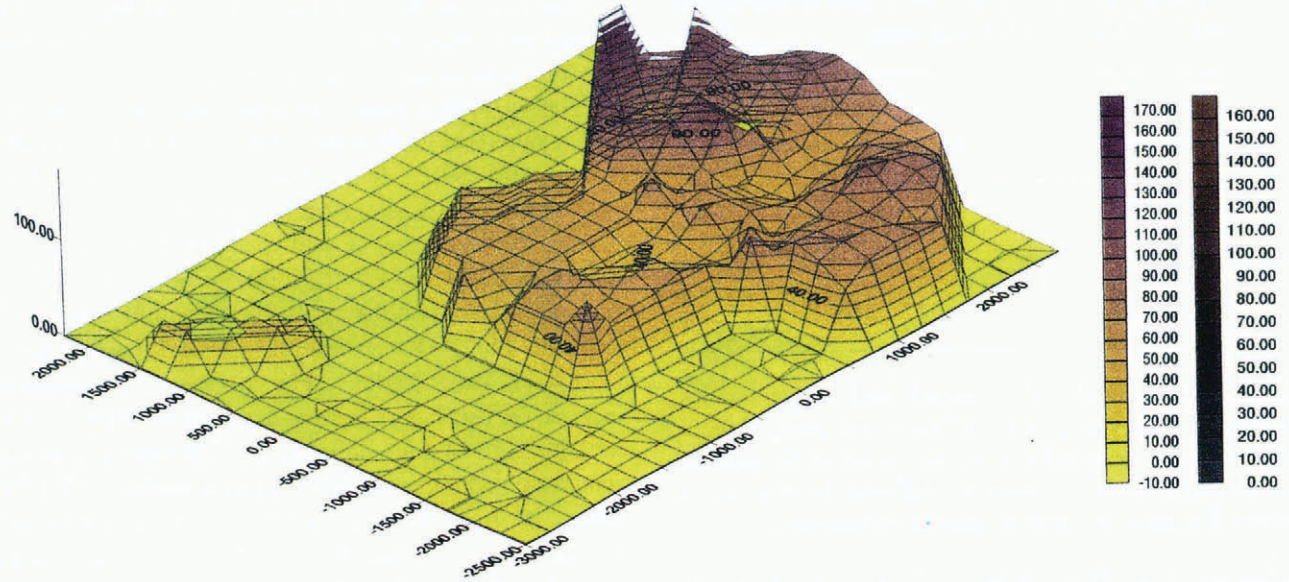

Fig. 7. Antarctic map of distribution of the ^{137}Cs.

b. ^{90}Sr

A zero correlation coefficient of ^{90}Sr vs temperature mainly caused by the lack of a relationship in the case of three samples J9, D50, D72, with low ^{90}Sr (110 Bq m^{-2}), masks a linear relation with a correlation coefficient around 0.90 for the six samples which have ^{90}Sr above 140 Bq m^{-2}. At two stations (J9 and D80), where we have measurements of both ^{90}Sr and ^{137}Cs, the $^{90}Sr/^{137}Cs$ ratio is respectively 1.1 and 2.1 (mean values: 1.6). These ratios do not differ from the global atmospheric ratio of 1.6 (Volchok and others, 1971; Eisenbud, 1987) and it is not possible to deduce a possible fractionation between these two radionuclides. Eight stations analysed both for ^{210}Pb and ^{90}Sr show a correlation of 0.89.

c. ^{210}Pb

The atmospheric concentration of ^{210}Pb, a long-lived daughter radionuclide (half-life 22.3 years) of radon, in the atmosphere depends on its rate of production through radon decay and its removal by atmospheric scavenging processes. The lack of radon sources in Antarctica and the time required for air to move from continental areas to this region results in a low radon (and its daughter nuclides) concentration in Antarctica.

The origin of ^{210}Pb over Antarctica has been widely discussed. Lambert and others (1966) suggested an essentially stratospheric origin for ^{210}Pb at the South Pole, based on a good correlation between ^{210}Pb and fission products over the South Pacific and Antarctica, but Lambert and others (1983) stated a tropospheric origin for ^{210}Pb. Based on the correlation between ^{210}Pb and the stratospheric radionuclides ^{7}Be and ^{137}Cs (and a high level of ^{210}Pb at the South Pole compared to Punta Arenas), Maenhaut and others (1979) suggested transport of ^{210}Pb to the interior of Antarctica through the lower stratosphere and (or) upper troposphere during the austral summer. The almost equal residence time of 5.5 days of ^{210}Pb and ^{222}Rn over the sub-Antarctic ocean, for the whole troposphere, suggests rapid transport of these radionuclides from their remote continental source; this transport of nuclides from mid latitudes towards Antarctica is not through the lower troposphere (Lambert and others, 1990).

In firn, the total of amount of ^{210}Pb (A) is the result of equilibrium between atmospheric flux (Φ) and radioactive decay after deposition. With a constant atmospheric flux, we have relation (6)

$$\Phi = \lambda \times A \qquad (6)$$

where λ is the radioactive constant of ^{210}Pb.

The fluxes are calculated from the continuous vertical profiles of ^{210}Pb concentration. The quantities measured in each of the samples along the profile are summed and relation (6) is used to convert the deposition in flux. Another method of determining fluxes would involve extrapolation of the different values measured in the profile to the surface. In order to deduce a mean concentration, C at the snow surface is linked to the flux by relation (7)

$$\Phi = C \times P \qquad (7)$$

where P represents the mean net accumulation on the site. The observed fluxes vary from 0.9 at 8.2 Bq m^{-2} a^{-1}, a value quite comparable to those obtained by Roos and others (1994) from lichens, mosses, grass, soil and lake sediments collected on the South Shetland Islands (3.8–17.5 Bq m^{-2} a^{-1}, with a mean of 8.6 Bq m^{-2} a^{-1}). These fluxes are strongly correlated with the accumulation (relation (8) with $\rho = 0.80$ (significant at the 99% confidence level).

$$Y(^{210}Pb) = 0.01164X\,(\text{accum.}) + 1.2785\,. \qquad (8)$$

The active volcano Mount Erebus has been believed to be responsible for the elevated concentrations in McMurdo Sound (Crozaz and others, 1964). The apparently high level at Roi Baudoin Station is due to the elevated snow-accumulation rate at this station.

The correlation coefficient of −0.74 between elevation and ^{210}Pb flux is in fact stronger (−0.80) for the 17 sites above 1000 m where the linear negative behaviour is obvious. The dry fall-outs for ^{210}Pb are lower than those for ^{137}Cs and, for all the stations, represent about 40% of the flux. The dispersion of values is significantly lower than for artificial radionuclides. Artificial radionuclide fluxes are discontinuous, whereas the natural flux from ^{210}Pb is continuous and the concentrations in adjacent samples are very similar. The measurements are not consistently affected by drift redistri-

https://doi.org/10.3189/S0022143000035024 Published online by Cambridge University Press

bution but in the case of occasional or discontinuous phenomena (nuclear tests, industrial accidents, volcanic events) it would be necessary to ensure representation of the sampling.

The spatial investigations of ^{210}Pb, based on 23 stations, reveals surprisingly well-defined structures on the omnidirectional variogram (Fig. 6b), with a clearly modelled growth up to the sill reached for a distance of 1100 km. The ^{210}Pb stations were clustered either in the line starting at Dumont d'Urville or on the Antarctic Plateau and along the coast. The directional variogram (Fig. 6a) for NNW110 (Dumont d'Urville line) shows a smaller range at 700 km, thus providing better information than the larger grid of the other measures. One hundred and sixty-two blocks of 250 km × 250 km were estimated for ^{210}Pb (Fig. 8). However, the map is purely indicative, due to the limited number of stations available. The second population of blocks above 2.5 Bq m^{-2} a^{-1} is clearly related to the scarp edges at the circumference of the continent. This is consistent with both the correlation coefficient of ^{210}Pb with altitude and the 0.57 correlation coefficient with latitude.

d. Tritium

The data for tritium fall-out are given as the total amount of tritium deposited between 1955 and 1980 along the DDu–DC axis, South Pole and Ross Ice Shelf (Table 1a). The tritium is incorporated in water vapour as HTO and most of the tritium present in Antarctica between 1955 and 1980 is due to atmospheric testing of fusion bombs which injected tritium into the stratosphere. The tritium deposition in Antarctica is strongly influenced by seasonal cycles and smoothing of the seasonal variations occurs by diffusion in the vapour phase during firnification (Merlivat and others, 1977; Jouzel and others, 1979a). The tritium fall-out over Antarctica varies from 211 to 840 TU m of water (1 TU = 118 Bq l^{-1}) and the average is 529 TU m of water. A plot of total tritium content vs rate of accumulation in seven stations along DDu–DC shows a good positive correlation of 0.84, suggesting a regular increase in tritium deposition with the increase in rate of accumulation. Despite the first values for very small lag distances h around 50 km, the four subsequent variogram values for 500, 800 km, etc. are consistent. The variogram with nine stations can surprisingly be modelled.

The station on the Ross Ice Shelf, which is 450 km from the coast but at 50 m elevation, is depleted in tritium compared to other stations. This suggests that moist air might have picked up the tritium from the surface and redistributed it elsewhere by eddy diffusion. The substantially higher tritium content, by a factor of 2, at the South Pole indicates preferential injection directly from the stratosphere (or opening of the stratosphere) by the direct vapour exchange of the tropospheric air mass with the stratospheric mass. However, for the preferential tritium fall-out at the South Pole, Jouzel and others (1979a) suggested that, because of the growth of stratospheric clouds and their precipitation in the higher troposphere (Stanford, 1973), a significant percentage of tritium-rich stratospheric water could be removed from the stratosphere and accounts for large tritium injections during the Antarctic winter at the South Pole. This stratospheric cloud-formation mechanism could have played a particular role during 1973 for which the very high tritium fall-out is not related to the nuclear explosion calendar but is the coldest year at these levels for the 1954–78 period (−84°C) (Jouzel and others, 1979a). However, a link with nuclear testing cannot be discarded (the fact that the 1973 French explosions produced a relatively large amount of debris has recently been disclosed).

The deposition of tritium over Antarctica is strongly related to mixing within the stratosphere and the processes of precipitation from the troposphere. The tritium formed at upper levels is brought down from higher stratospheric altitudes within the circumpolar vortex and then is passed into the troposphere by vertical exchange processes over the polar regions during the Antarctic winter when no temperature inversion exists at the South Pole tropopause. When these particular conditions exist, a continuous rapid exchange of air between the lower polar stratosphere and the troposphere possibly occurs (Martell, 1970). Tritium concen-

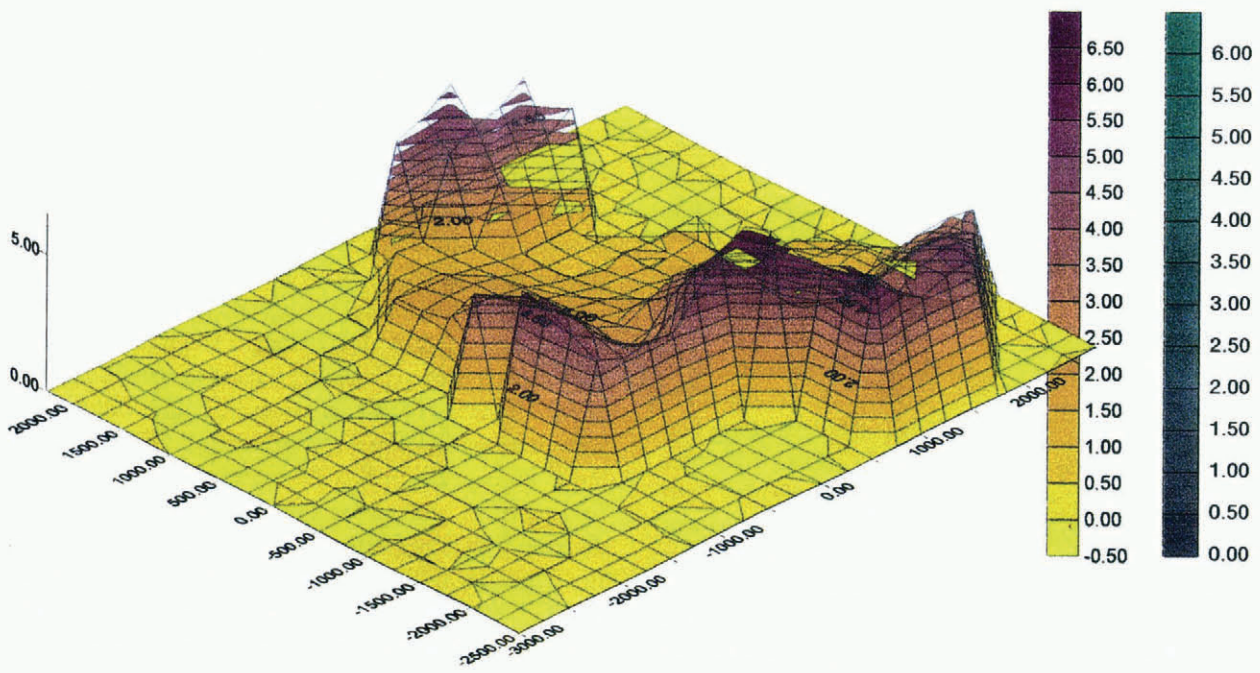

Fig. 8. Antarctic map of distribution of the ^{210}Pb.

https://doi.org/10.3189/S0022143000035024 Published online by Cambridge University Press

tration in the Antarctic precipitation is much higher than in precipitation at temperate southern latitudes. Koide and others (1979) suggested this was due to the diluting influence of the ocean at most intermediate latitude stations and that continental effects are very important in understanding tritium deposition.

Finally, we note two interesting features of tritium fall-out. First, the latitudinal and seasonal dependence of this fall-out shows similarities between natural (analysed on snow fallen before the first nuclear testing) and artificial tritium; these similarities show that the same mechanisms govern the deposition of artificial and natural tritium (Jouzel and others, 1982). Secondly, the seasonal patterns of tritium and β fall-out clearly differ, with the maxima occurring respectively during the Antarctic winter and Antarctic summer. According to Taylor (1968), this is due to the different transfer mechanisms involved. β products are transported with particular material in the lower stratosphere and enter the stratosphere at mid latitudes (seasonal fall-out variation characterized by a summer maximum), whereas tritium, formed at higher levels, is brought down from higher stratospheric altitudes within the circumpolar vortex and is then passed into the troposphere over the polar regions during the Antarctic winter.

e. Other radionuclides

The inventories of ^{241}Pu and $^{239-240}$Pu are roughly similar for DC and station J9 on the Ross Ice Shelf (Table 1b). The ^{238}Pu/$^{239-240}$Pu ratio is in good agreement with the values obtained from lichens, mosses, grass and soil collected on the South Shetland Islands (Roos and others, 1994) or in the McMurdo Sound area and around Syowa Station (Hashimoto and others, 1989). ^{241}Am inventory at the South Pole and DC also agrees with the South Shetland Islands inventory but disagrees with ^{241}Pu at DC and the Ross Ice Shelf: at DC, ^{241}Am, a daughter product of ^{241}Pu represents at the date of measurement (1992) less than 3% of ^{241}Pu. Koide and others (1979) suggested for ^{238}Pu a major contribution to the SNAP-9A event in 1964 and for ^{241}Pu the reflection of the Mike, Yvy and early American thermonuclear tests, characterized by their very high ratio of ^{241}Pu/$^{239-240}$Pu : 27 in 1953 compared to a global world ratio of 13 (Roos and others, 1994).

The fluxes of cosmogenic-produced ^{10}Be are higher by a factor of about 2 at the South Pole (2.7) compared to DC (1.6). The ratio of ^{10}Be between the South Pole and DC is not similar to the ratio of accumulation for these two stations. This difference may be due to dry fall-out. If we assume the same concentration of ^{10}Be in snowfall at these two stations, dry fall-outs are respectively 30% and 50% at the South Pole and DC.

^{234}Th (0.012 Bq m^{-2} a^{-1}) and ^{226}Ra (0.082 Bq m^{-2} a^{-1}) flux (decay products of the ^{238}U family) are reported for the first time at DC. ^{234}Th is a short-lived radionuclide (24 days) in secular equilibrium with ^{238}U. The ^{226}Ra flux (the long-lived radionuclide before radon) is about 7% of the total ^{210}Pb flux. After deposition, this ^{226}Ra produces ^{210}Pb in snow, with apparent radioactive decay of ^{226}Ra (~1600 years). In 60 year old snow, the activity of this ^{210}Pb is the same as the remaining activity of ^{210}Pb incorporated in snow by direct atmospheric scavenging (6%). For the last century, snow dating using ^{210}Pb is easy but ^{210}Pb supported by ^{226}Ra should not be neglected.

A comparison between the artificial (^{137}Cs, ^{90}Sr, ^{3}H), terrigenous (^{210}Pb, ^{234}Th, ^{226}Ra) and cosmogenic (^{10}Be) radionuclides indicates that artificial radionuclides constitute more than 90% of the total long-lived radionuclides deposited in Antarctica during the 1955–80 period.

4. DISCUSSION

Most thermonuclear tests increased the radionuclide debris of the Northern Hemisphere's troposphere and stratosphere. While tropospheric radionuclide debris deposited quickly on the Earth's surface, the stratospheric debris began to mix. After the initial tropospheric input had been deposited, deposition over Antarctica was primarily from stratospheric input. The Southern Polar troposphere received a much smaller initial artificial radionuclide input from thermonuclear tests. Most of the radionuclides it received came from the stratosphere. This idea can also be substantiated by radio-isotope measurements performed in Antarctica (Picciotto and Wilgain, 1963; Crozaz, 1969; Taylor, 1968) and by the 1.5 years residence time suggested by Pourchet and others (1983). The arrival of artificial radionuclides is in December and January when opening of the stratosphere takes place. A pronounced maximum deposition in the Antarctic summer has been illustrated for ^{3}H (Jouzel and others, 1979b) and ^{137}Cs (Lockhart and others, 1965), suggesting that the Southern Hemisphere does undergo seasonal variations in stratospheric–tropospheric exchange such as observed in the Northern Hemisphere. Jouzel and others (1979a) suggested a 2 year delay for the arrival of tritium at the South Pole after its production in the Northern Hemisphere and noted the existence of high values in South Polar snow.

The estimated dry fall-out is 82, 60 and 40% for ^{137}Cs, ^{90}Sr and ^{210}Pb, respectively. These dispersed values can be explained by the geographical heterogeneity of the sampling and by the low number of common measurements. The similar origin for ^{137}Cs and ^{90}Sr should result in the same percentage of dry fall-out for these two radionuclides. We therefore attribute the observed differences to the uncertainty of the determinations. For ^{210}Pb, the smaller value may reflect the arrival, from the surrounding continents, of a tropospheric fraction directly incorporated in the clouds. The tritium case is also different and the explanation for 70% of the apparent dry fall-out may be the effect of the direct molecular vapour exchange of atmospheric air masses with stratospheric masses. The observed difference between radionuclides should be applied for a classification of transport processes concerning stable species.

The omnidirectional variograms for ^{137}Cs show "noise", (nugget effect) equivalent to half of the statistical variance. This noise is due to the low representativeness of a snow core in the estimation of discontinuous flux. This will result in an inaccurate estimation and mapping of ^{137}Cs. Unlike ^{137}Cs, the ^{210}Pb deposition flux fluctuates little or none and the "nugget effect" associated with this radionuclide is smaller than for ^{137}Cs (6%). A local variation in transport, accumulation and dry fall-out at high-altitude inland stations, such as DC, DB and Vostok, or preferential injection directly from the stratosphere at the South Pole (for tritium) are the most probable causes for variation in the distribution of radionuclides (^{137}Cs and ^{90}Sr) at these stations.

ACKNOWLEDGEMENTS

Financial assistance to S. K. B., provided by the Department of Science and Technology, Government of India, under the BOYSCAST fellowship, accorded to S. K. Bartarya, is gratefully acknowledged. Investigations at Livingston Island were made possible by Proyecto CICYT ANT 93.

REFERENCES

Bendezu, A. M. 1978. Application des mesures de plomb 210 et Sr-90 à l'étude des èchanges entre l'atmosphère et la calotte Antarctique. (Ph.D. thesis, Université de Paris.)

Crozaz, G. 1967. Mise au point d'une méthode de datation des glaciers basée sur la radioactivité du Pb-210. (Thèse de doctorat, Université Libre de Bruxelles.)

Crozaz, G. 1969. Fission products in Antarctic snow: an additional reference level in January, 1965. *Earth Planet. Sci. Lett.*, **6**(1), 6–8.

Crozaz, G., E. Picciotto and W. de Breuck. 1964. Antarctic snow chronology with Pb^{210}. *J. Geophys. Res.*, **69**(12), 2597–2604.

Cutter, G. A., K.W. Bruland and R.W. Risebrough. 1979. Deposition and accumulation of plutonium isotopes in Antarctica. *Nature*, **279**(5714), 628–629.

Delmas, R. and M. Pourchet. 1977. Utilisation de filtres échangeurs d'ions pour l'étude de l'activité β globale d'un carottage glaciologique. *International Association of Hydrological Sciences Publication* 118 (Symposium at Grenoble 1975 — *Isotopes and Impurities in Snow and Ice*), 159–163.

Eisenbud, M. 1987. *Environmental radioactivity from natural, industrial and military sources.* San Diego, CA, Academic Press Inc.

Feely, H.W., H. Seitz, R. J. Lagomarsino and P. E. Biscaye. 1966. Transport and fallout of stratospheric radioactive debris. *Tellus*, **18**(2–3), 316–328.

Giovinetto, M. B., N. M. Waters and C. R. Bentley. 1990. Dependence of Antarctic surface mass balance on temperature, elevation, and distance to open ocean. *J. Geophys. Res.*, **95**(D4), 3517–3531.

Goodwin, I. D. 1990. Snow accumulation and surface topography in the katabatic zone of eastern Wilkes Land, Antarctica. *Antarct. Sci.*, **2**(3), 235–242.

Goodwin, I. D. 1991. Snow-accumulation variability from seasonal surface observations and firn-core stratigraphy, eastern Wilkes Land, Antarctica. *J. Glaciol.*, **37**(127), 383–387.

Graf, W. *and 6 others*. 1994. Snow-accumulation rates and isotopic content (^2H, ^3H) of near-surface firn from the Filchner–Ronne Ice Shelf, Antarctica. *Ann. Glaciol.*, **20**, 121–128.

Hashimoto, T., T. Morimoto, Y. Ikeuchi, K. Yoshimizu, T. Torii and K. Komura. 1989. A survey of artificial radionuclides in the Antarctic. *Radioisotopes*, **38**, 209–218.

Jouzel, J., M. Pourchet, C. Lorius and L. Merlivat. 1979a. Artificial tritium fallout at the South Pole. *In Behaviour of tritium in the environment*. Vienna, International Atomic Energy Agency, 31–46. (SM 232/38.)

Jouzel, J., L. Merlivat, M. Pourchet and C. Lorius. 1979b. A continuous record of artificial tritium fallout at the South Pole (1954–1978). *Earth Planet. Sci. Lett.*, **45**(1), 188–200.

Jouzel, J., L. Merlivat, D. Mazaudier, M. Pourchet and C. Lorius. 1982. Natural tritium deposition over Antarctica and estimation of the mean global production rate. *Geophys. Res. Lett.*, **9**(10), 1191–1194.

Junge, C. C. 1963. *Air chemistry and radioactivity*. New York, Academic Press.

Koide, M. and E. D. Goldberg. 1981. $^{241}Pu/^{239+240}Pu$ ratios in polar glaciers. *Earth Planet. Sci. Lett.*, **54**(2), 239–247.

Koide, M., R. Michel, E. D. Goldberg, M. Herron and C. C. Langway, Jr. 1979. Depositional history of artificial radionuclides in the Ross Ice Shelf, Antarctica. *Earth Planet. Sci. Lett.*, **44**(2), 205–223.

Kolb, W. 1970. Jahreszeitliche Schwankungen der $7Be^-$, $54Mn^-$ und Spaltprodukt-Konzentrationen der bodennahen Luft. *Tellus*, **22**(4), 443–450.

Lambert, G., B. Ardouin, M. Nezami and G. Polian. 1966. Possibilities of using lead 216 as an atmospheric tracer. *Tellus*, **18**(2–3), 421–426.

Lambert, G., B. Ardouin, J. Sanak, C. Lorius and M. Pourchet. 1977. Accumulation of snow and radioactive debris in Antarctica: a possible refined radiochronology beyond reference levels. *International Association of Hydrological Sciences Publication* 118 (Symposium at Grenoble 1975 — *Isotopes and Impurities in Snow and Ice*), 146–158.

Lambert, G., B. Ardouin and A. Mesbah-Bendezu. 1983. Atmosphere to snow transfer in Antarctica. *In* Pruppacher, H. R., R. G. Semonin and W. G. N. Slinn, *eds. Precipitation scavenging, dry deposition, and resuspension.* New York, Elsevier Science Publishers, 1289–1300.

Lambert, G., B. Ardouin and J. Sanak. 1990. Atmospheric transport of trace elements towards Antarctica. *Tellus*, **42B**(1), 76–82.

Lockhart, L.B., Jr, R.L. Patterson and A.W. Saunders, Jr. 1965. *Atmospheric radioactivity in Antarctica 1959–1963.* Washington, DC, U.S. Naval Research Laboratory. (Report 6341.)

Luyanas, V. Yu., R. Yu. Yasyulyonis, D. A. Shopauskiene and B. I. Styra. 1970. Cosmogenic ^{22}Na, ^7Be, ^{32}P, and ^{33}P in atmospheric dynamics research. *J. Geophys. Res.*, **75**(18), 3665–3667.

Maenhaut, W., W. H. Zoller and D. G. Coles. 1979. Radionuclides in the South Pole atmosphere. *J. Geophys. Res.*, **84**(C6), 3131–3138.

Martell, E. A. 1970. Transport patterns and residence times for atmospheric trace constituents versus altitude. *Adv. Chem. Ser.*, **93**, 138–157.

Merlivat, L., J. Jouzel, J. Robert and C. Lorius. 1977. Distribution of artificial tritium in firn samples from East Antarctica. *International Association of Hydrological Sciences Publication* 118 (Symposium at Grenoble 1975 — *Isotopes and Impurities in Snow and Ice*), 138–145.

Moore, H. E., S. E. Poet and E. A. Martell. 1973. ^{222}Rn, ^{210}Pb, ^{210}Bi and ^{210}Po profiles and aerosol residence times versus altitude. *J. Geophys. Res.*, **78**(30), 7065–7075.

Morgan, V. I., I. D. Goodwin, D. M. Etheridge and C. W. Wookey. 1991. Evidence from Antarctic ice cores for recent increases in snow accumulation. *Nature*, **354**(6348), 58–60.

Pettre, P., J. F. Pinglot, M. Pourchet and L. Reynaud. 1986. Accumulation distribution in Terre Adèlie, Antarctica: effect of meteorological parameters. *J. Glaciol.*, **32**(112), 486–500.

Picciotto, E. and S. Wilgain. 1963. Fission products in Antarctic snow, a reference level for measuring accumulation. *J. Geophys. Res.*, **68**(21), 5965–5972.

Pinglot, J. F. and M. Pourchet. 1979. Low-level beta counting with an automatic sample changer. *Nucl. Instrum. Methods*, **166**(3), 483–490.

Pinglot, J. F. and M. Pourchet. 1994. Spectrométrie gamma á très bas niveau avec anti-Compton NaI (Tl), pour l'étude des glaciers et des sédiments. *CEA Note* 2756, 291–296. (Journeeś des Spectrométrie Gamma et X 93, CEA-DAMRI, 12–14 October 1993, Paris, France.)

Poet, S. E., H. E. Moore and E. A. Martell. 1972. Lead 210, bismuth 210, and polonium 219 in the atmosphere: accurate ratio measurements and application to aerosol residence time determination. *J. Geophys. Res.*, **77**(33), 6515–6527.

Pourchet, M., J. F. Pinglot and C. Lorius. 1983. Some meteeorological applications of radioactive fallout measurements in Antarctic snows. *J. Geophys. Res.*, **88**(C10), 6013–6020.

Raisbeck, G. M. *and 6 others*. 1981. Cosmogenic ^{10}Be concentrations in Antarctic ice during the past 30,000 years. *Nature*, **292**(5826), 825–826.

Raisbeck, G. M., F. Yiou, D. Bourles, C. Lorius, J. Jouzel and N. I. Barkov. 1987. Evidence for two intervals of enhanced ^{10}Be deposition in Antarctic ice during the last glacial period. *Nature*, **326**(6110), 273–277.

Raisbeck, G. M., F. Yiou, J. Jouzel and J. R. Petit. 1990. ^{10}Be and δ^2H in polar ice cores as a probe of the solar variability's influence on climate. *Philos. Trans. R. Soc. London, Ser. A*, **330**(1615), 463–470.

Rama. 1963. Atmospheric circulation from observations of natural radioactivity. *J. Geophys. Res.*, **68**(13), 3861–3866.

Reiter, E. R. 1978. *Atmospheric transport processes (Pt-4): radioactive tracers.* Springfield, VA, U.S. Department of Energy. Technical Information Center. (D.O.E. Critical Review Series.)

Roos, P., E. Holm, R. B. R. Persson, A. Aarkrog and S. P. Nielsen. 1994. Deposition of ^{210}Pb, ^{137}Cs, $^{239+240}Pu$, and ^{241}Am in the Antarctic Peninsula area. *J. Environ. Radioactivity*, **24**, 235–251.

Sanak, J. 1983. Contribution à l'étude du transport des aérosols d'origine continentale vers l'Antarctique. (Thèse de doctorat, Université Pierre et Marie Curie, Paris.)

Stanford, J. L. 1973. Possible sink for stratospheric water at the winter Antarctic pole. *J. Atmos. Sci.*, **30**, 1431–1436.

Taylor, C. B. 1968. A comparison of tritium and strontium-90 fallout in the Southern Hemisphere. *Tellus*, **20**(4), 559–576.

Telegadas, K. 1972. Atmospheric radioactivity along the HASL ground-level sampling network, 1968 to mid-1970, as an indicator of tropospheric and stratospheric sources. *J. Geophys. Res.*, **77**(6), 1004–1011.

Volchok, H. L., V. T. Bowen, T. R. Folson, W. S. Broecker, E. A. Schwart and G. S. Bien. 1971. Oceanic distribution of radionuclides from nuclear explosions. *In Radioactivity in the marine environment*. Washington, DC, U.S. National Academy of Sciences, 42–89.

Wilgain, S., E. Picciotto and W. de Breuck. 1965. Strontium 90 fallout in Antarctica. *J. Geophys. Res.*, **70**(24), 6023–6032.

Young, N.W., M. Pourchet, V. M. Kotlyakov, P. A. Korolev and M. B. Dyurgerov. 1982. Accumulation distribution in the IAGP area, Antarctica: 90° E–150° E. *Ann. Glaciol.*, **3**, 333–338.

MS received 12 October 1993 and accepted in revised form 28 April 1997